Available online at www.sciencedirect.com

ScienceDirect

Procedia Engineering 69 (2014) 678 – 685

Procedia Engineering

www.elsevier.com/locate/procedia

24th DAAAM International Symposium on Intelligent Manufacturing and Automation, 2013

Effect of Tenon Length on Flexibility of Mortise and Tenon Joint

Seid Hajdarević*, Sandra Martinović

University of Sarajevo, Mechanical Engineering Faculty, Vilsonovo setaliste 9, Sarajevo 71000, Bosnia and Herzegovina

Abstract

This paper presents numerical analysis of the effects of tenon length on flexibility of mortise and tenon joints. Numerical calculations are carried out with a linear elastic model for orthotropic material. The mathematical model is solved by a finite element method. The results of the calculation indicate that a mortise and tenon joint becomes stiffer as tenon length increases. A satisfactory agreement was found between the experimental data taken from literature and the obtained results, thus confirming the conclusions made. Rotation stiffness was determined and also used in the structural analysis of a simple furniture frame. The results revealed that stiffness of joints in a frame had a considerable impact on the structure deflection.

Keywords: wood; mortise and tenon joint; finite element method; stiffness

1. Introduction

Frame structure represents the most widely used type of furniture constructions. Common construction is manufactured by connecting wood elements with shape-adhesive joints. The stiffness and strength of frame structure depend on the properties of the involved joints. In order to be able to carry out the analysis and optimization of construction it is necessary to know the properties of the joints. Attempts are being made toward analysis and finding solutions that would improve the properties of the joints. The studied literature has established that investigations are focused on the numerical determination of stress and strain in both tenon and dowel joints. Distribution of stresses in glue lines of wooden joints subjected to shearing, torsion, and bending were analyzed by several authors [1-5]. Mihailescu [6] used finite element methods to compare the stress and deflections in both square and round mortise and tenon joints. Deformability in tenon and mortise joints is investigated by Eckelman.

* Corresponding author. Tel.: +387-33-729-824; fax: +387-33-653-055.
E-mail address: hajdarevic@mef.unsa.ba

doi:10.1016/j.proeng.2014.03.042

He first introduced the semi-rigid joint concept into furniture joint stiffness analysis [7]. Deformability and bending stress in tenon and mortise joints were experimentally investigated by Erdil [8]. The above studies presented a comprehensive expression that reflects the functional relationship of variables such as wood species, adhesives and joint geometry, on the properties of the joint.

2. Research objective and methodology

In the common structural analysis of a furniture frame, joints are modeled by considering certain idealizations. Joints are assumed to be ideally rigid or pinned. In fact, most joints in real wood structures are more or less flexible or semi-rigid [9]. Tangents to the elastic curves of the sections framing into a joint at the point of intersection do change as the joint is loaded, Fig. 1a. The moment is dependent on the function of relative rotation between structural elements connected to the same joint, Fig. 1b. If the relationship between the angle change and the moment is linear, this relationship is commonly described by the constant Z, where: $Z=\phi/M$ [8].

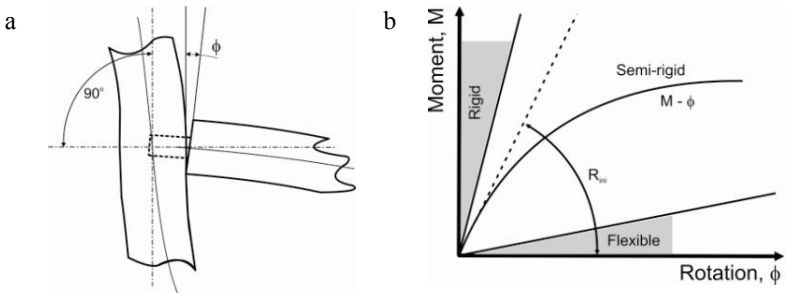

Fig. 1. (a) semi-rigid joint; (b) moment-rotation curves.

The aim of this study was to verify the numerical calculations describing the effect of joint geometry on the flexibility of furniture joints. This study employed a numerical method for the analysis of mortise and tenon joint stiffness with an objective to determine the effects of tenon length on flexibility of mortise and tenon T-type joints. The obtained estimates of rotational stiffness are used in the structural analysis of a simple frame structure in order to determine the influence of joint properties on the stiffness of wooden constructions.

Physical model (configuration, measurements and material, except type of glue) of joints and a loading diagram used in this study are borrowed from literature [8]. Results of rotational stiffness obtained in this study are compared with experimental values.

2.1. Mathematical model

The equation of momentum balance, expressed in the Cartesian tensor notation [10]

$$\int_S \sigma_{ij} n_j dS + \int_V f_i dV = 0 \tag{1}$$

and of the constitutive relation for the elastic material

$$\sigma_{ij} = C_{ijkl}\varepsilon_{kl} = \frac{1}{2} C_{ijkl}\left(\frac{\partial u_k}{\partial x_l} + \frac{\partial u_l}{\partial x_k}\right) \tag{2}$$

describe the stress and strain of a loaded solid body in static equilibrium. In the equations above, x_j are Cartesian spatial coordinates, V is the volume of solution domain bounded by the surface S, σ_{ij} is the stress tensor, n_j is the outward unit normal to the surface S, f_i is the volume force, C_{ijkl} is the elastic constant tensor components, ε_{kl} is the strain tensor, and u_k represents the point displacement. Equation (2) for the elastic, orthotropic material can be expressed in the following matrix form

$$\begin{bmatrix} \sigma_{xx} \\ \sigma_{yy} \\ \sigma_{zz} \\ \sigma_{xy} \\ \sigma_{xz} \\ \sigma_{yz} \end{bmatrix} = \begin{bmatrix} A_{ij} \end{bmatrix} \begin{bmatrix} \varepsilon_{xx} \\ \varepsilon_{yy} \\ \varepsilon_{zz} \\ \varepsilon_{xy} \\ \varepsilon_{xz} \\ \varepsilon_{yz} \end{bmatrix}. \tag{3}$$

Twelve non-zero orthotropic elastic constants A_{ij} are related to the Young's modulus E_i, the Poisson's ratio ν_{ij} and the shear modulus G_{ij}.

In order to complete the mathematical model, the boundary conditions have to be specified. The surface traction f_{Si} and/or the displacement u_S at the domain boundaries are known, i.e.

$$\sigma_{ij} n_j = f_{S_i} \quad \text{and} \quad u_i = u_S. \tag{4}$$

Governing equations (1) combined with the constitutive relations (2) are solved through a numerical method based on the finite element. Calculations in this study were performed by using the CATIA software package.

2.2. Physical model

Rectangular mortise and tenon joint was selected for investigation. Geometries and measurements of the T-type end to side grain joints are shown in Fig. 2. and Tab. 1. All variables except tenon length were held constant. Tenon length varied from 12.7 mm to 50,8 mm.

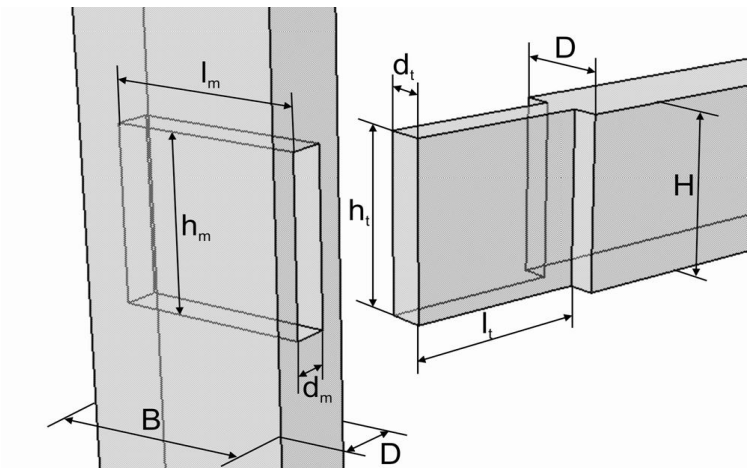

Fig. 2. Mortise and tenon joint geometries.

Table 1. Mortise and tenon joint measurements.

Post and rail dimensions, mm			Tenon dimensions, mm			Mortise dimensions, mm		
B	H	D	h_t	d_t	l_t	h_m	d_m	l_m
76,2	50,8	25,4	50,8	9,5	12,7 19,05 25,4 38,1 50,8	51	9,7	l_t+3,87

A 0,1 mm thick gap was placed between the tenon and the mortise in which a glue bond was formed. The shoulder of the tenon (rail) was contact connected to the wall of the mortise (post). Calculation was carried out for maple wood (*Acer saccharum Marsh.*). Its elastic properties for wood density ρ=0,57 g/cm^3 and moisture content of 12% are presented in Tab. 2 [11]. Another material component is polyvinyl acetate (PVAC) glue. Selected elastic properties of the glue are E=465,74 MPa and ν=0,29 [1].

Table 2. Elastic properties of maple (*Acer saccharum Marsh.*).

Modulus of elasticity, GPa			Rigidity modulus, GPa			Poisson´s ratio					
E_L	E_R	E_T	G_{LR}	G_{LT}	G_{RT}	ν_{LR}	ν_{LT}	ν_{RT}	ν_{TR}	ν_{RL}	ν_{TL}
13,810	1,311	0,678	1,013	0,753	0,255	0,46	0,50	0,82	0,42	0,044	0,025

Loading diagram of mortise and tenon joints is shown in Fig. 3. The post of a joint was fixed at upper and lower end. Translation of the lateral surface points of the post was fixed in restrained direction *x*. Loaded end of the rail was at a distance of 304,8 mm from the face of the post. Appropriate value (1/3 of ultimate load [8]) of bending moment was transformed into shear stress on the cross-section surface of the rail. Values of the bending moment acting on the joint and appropriate shear stress are presented in Tab. 3

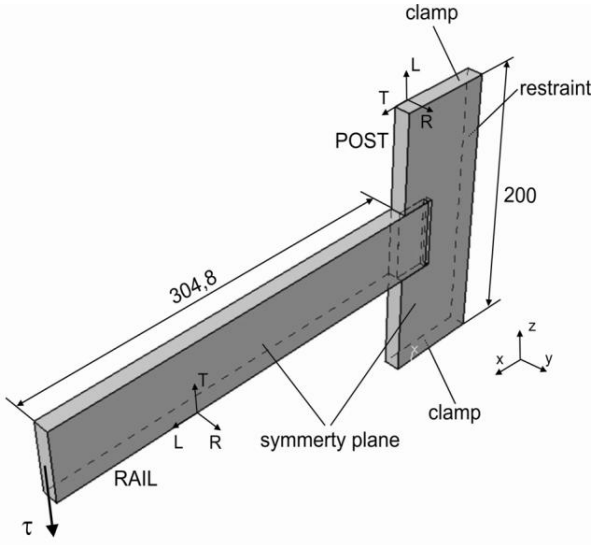

Fig. 3.Mortise and tenon joint loading diagram.

Keeping in mind the perpendicular position of the post and the rail in the global coordinate system, and the different direction of wood fibers resulting from this fact, two local coordinate systems were applied. Because of the symmetry, one half of the joint is taken for the solution domain.

Table3. Values of bending moment and shear stress.

Tenon length, mm	M, Nm	τ, MPa
12,7	65,05	0,165
19,05	106,67	0,271
25,4	133,34	0,339
38,1	170,86	0,434
50,8	221,82	0,564

3. Results

The results of the numerical calculation revealed that the tenon underwent rotation and deflection. Points at the upper tenon surface slipped outside the mortise and were moved downwards, while points at the bottom tenon surface slipped inside the mortise and moved downwards, Fig 4. The effect of the interaction between the rail and post is the result of bending of the tenon and torsion of the glue line.

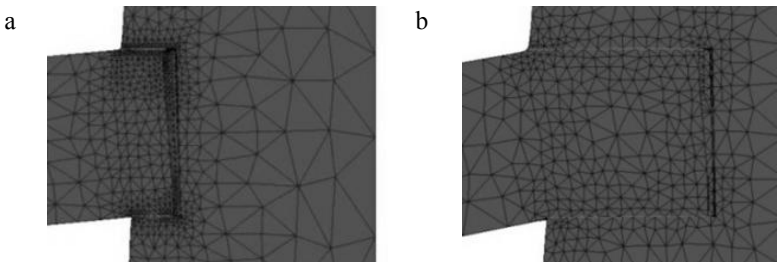

Fig. 4. Joint deformations: a) tenon length 12,7 mm, b) tenon length 50,8 mm, (symmetry plane; scale 20:1).

The effect of the point position in the upper and bottom shoulder edge of the tenon on the change in the point displacement was assessed. Position of the selected points is shown in Fig. 5 and *u* displacement results are presented in Tab.4. It is evident from Tab. 4 that the displacement of points in the outer plane is higher compared to point displacements in the symmetry plane.

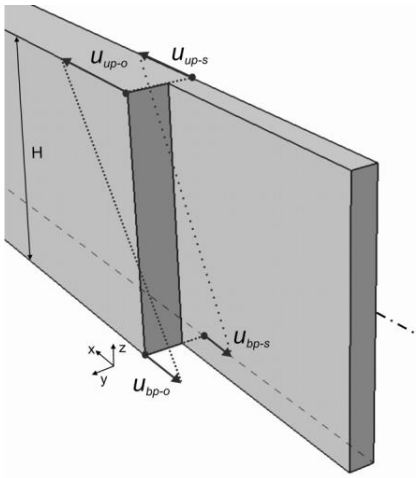

Fig. 5. Selected points position.

Table 4. u displacement of points in the upper and bottom edge of tenon shoulder.

Tenon length	*u* displacement of points			
	symmetry plane		outer plane	
	$u_{up\text{-}s}$	$u_{bp\text{-}s}$	$u_{up\text{-}o}$	$u_{bp\text{-}o}$
mm	mm	mm	mm	mm
12,7	0,0947	-0,0846	0,1214	-0,0892
19,05	0,1234	-0,1144	0,1641	-0,1275
25,4	0,1312	-0,1233	0,1792	-0,1418
38,1	0,1379	-0,1305	0,1965	-0,1498
50,8	0,1604	-0,1530	0,2343	-0,1903

The rotation that occurs in semi-rigid joints is described by rotational stiffness R, which is defined by the expression

$$R = \frac{M}{\phi} \tag{5}$$

where: ϕ is the angle change resulting from the joint behavior (radians), and M is the bending moment acting on the joint (Nm).

Angle change of selected joints was evaluated through the use of displacement results that are presented in Tab.4 and rail width, Fig.5. Values of the rotational stiffness were determined by means of the expression

$$R = \frac{H}{u_{up} + u_{bp}} \cdot M \tag{6}$$

where: u_{up} and u_{bp} represent the absolute values of the upper and bottom point *u* displacement (mm), H is the rail with (mm), and M is the bending moment acting on the joint (Nm).

The effect of tenon length on the change in rotational stiffness R was assessed. Values of rotational stiffness R for five tenon lengths are given in Tab. 5 and shown in Fig. 6. Description of the test and detailed experimental results can be found in [8].

Table 5. Rotational stiffness R - five tenon lengths.

Tenon length, mm	Rotational stiffness, Nm/rad				
	Exp. results*	Numerical results			
		symmetry plane	differ., %	outer plane	differ., %
12,7	13558,92	18432,08	35,94	15694,58	15,75
19,05	20837,17	22790,05	9,37	18579,23	-10,84
25,4	21793,64	26607,24	22,09	21101,65	-3,18
38,1	36183,16	32337,91	-10,63	25065,81	-30,73
50,8	29289,79	35951,61	22,74	26538,12	-9,39

* Experimental results are taken from [8]

These results indicate that the joint becomes increasingly stiffer as tenon length is increased. For tenon length 12,7 mm, the joint reached 46,3% (according to experimental results), 51% (symmetry plane) and 59% (outer plane) of the rotational stiffness which the joint would have if the tenon length was 50,8 mm. Differences between rotational stiffness obtained experimentally and from numerical calculation are ranged 9,37% to 35,94% (symmetry plane) and 15,75% to 30,73% (outer plane).

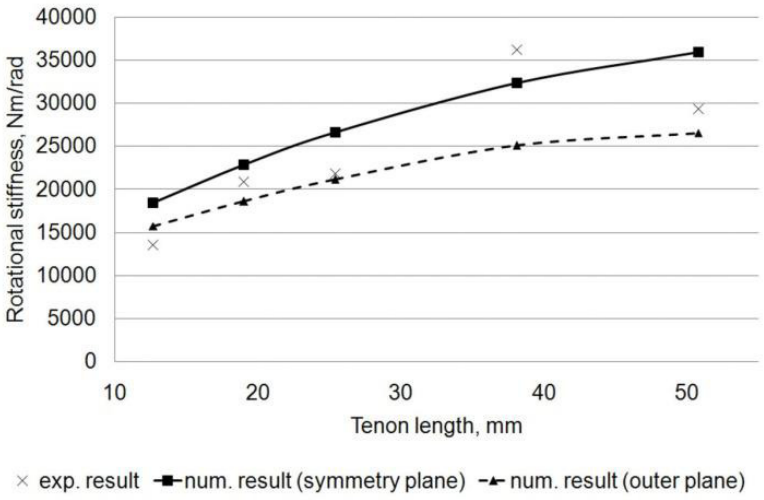

Fig. 6. Rotational stiffness R - five tenon lengths.

Rotational stiffness determined for the joints makes it possible to conduct more exact analyses of constructions that utilize these joints. An example presented below was used only in order to illustrate the consequence of the joint rotational stiffness implementation in the structural analysis of a statically indeterminate furniture frame.

Physical model of a frame and the loading diagram are shown in Fig. 7. Selected elastic properties of the material are E_L=13,81 GPa (longitudinal elastic modulus of maple) and ν=0,3. Beam elements (1D; transverse shear based on the Timoshenko theory) were employed for the modeling of structure. The connections are assigned as linear elastic rotational springs at beam-to-column joints. Spring rigidity at the ends of the frame element is defined by the rotational stiffness value obtained for symmetry plane, Tab. 5. The effect of the tenon length on the horizontal displacement change in the reference point C was assessed. Horizontal displacement in the point C for semi-rigid joints (five tenon lengths) and for rigid joints is shown in Fig. 8.

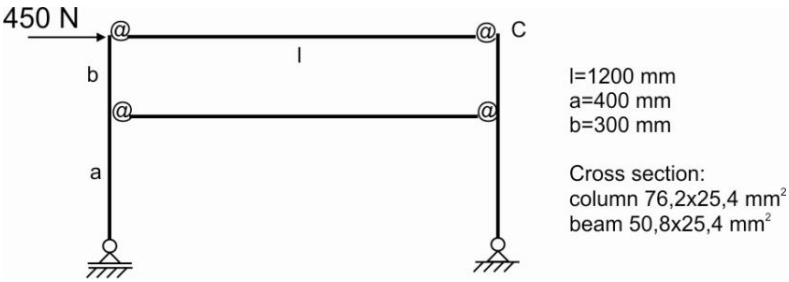

Fig. 7. Frame: physical model and loading diagram.

Results indicate that the structures become stiffer as tenon length is increased. For tenon length 50,8 mm, the point C reached 80% of the displacement it would have if the tenon length was 12,7 mm. Differences between displacement in the reference point C obtained for rigid and semi-rigid joints are ranged from -27% (tenon length 50,8 mm) to -42% (tenon length 12,7 mm).

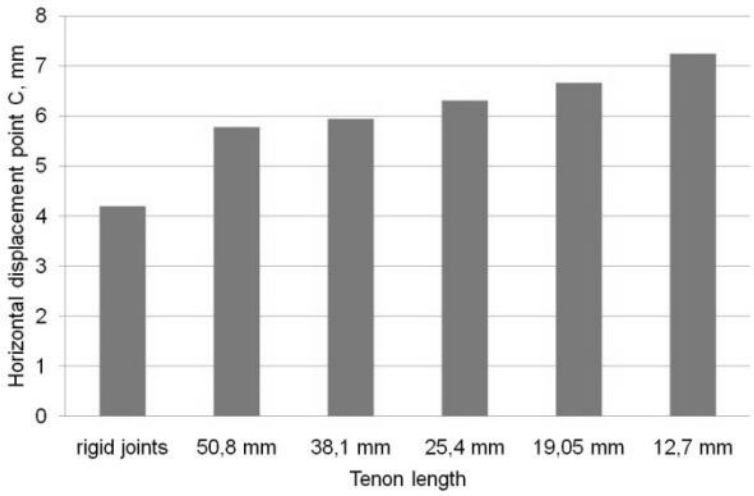

Fig. 8. Horizontal displacement point C for semi-rigid joints (five tenon lengths) and for rigid joints.

4. Conclusion

Based on the performed numerical calculations, several conclusions were drawn. It is evident from the analysis of rotational stiffness that the joints become stiffer as tenon length is increased. Similarity between experimental and numerical results of rotational stiffness allows for a conclusion that the research model was accurately designed. The stiffness of joints in a furniture frame has a considerable impact on the frame deformation.

The performed research revealed that the numerical procedure used in the study provides a convenient method of obtaining the information needed for determining rotational stiffness for shape-adhesive wood joints. The research model could be used for optimization of joints in wooden constructions. Many variables affecting the stiffness of joints could be evaluated individually or the interaction of variables on the properties of a joint could be analyzed. The next step will be to investigate the influence of joint properties on wood structure behavior under the service loads and implication on design improvements.

References

[1] J. Smardzewski, Effect of wood species and glue type on contact stresses in a mortise and tenon joint, Journal of Mechanical Engineering Science, (2008) 222(12), pp. 2293-2299.
[2] S. Prekrat, J. Smardzewski, M. Brezović, S. Pervan, Quality of corner joints of beech chairs under load, Drvna industrija, Vol. 63, No. 3 (2012), pp. 205-210.
[3] I. Horman, S. Hajdarević, S. Martinović, N. Vukas, Numerical Analysis of Stress and Strain in a Wooden Chair, Drvna industrija, Vol. 61, No.3 (2010), pp. 151-158.
[4] I. Horman, S. Hajdarević, S. Martinović, N. Vukas, Stiffness and strenght analysis of corner joint, TTEM, Vol.5, No.1(2010), pp. 48-53.
[5] S. Hajdarević, Š. Šorn, Effect of the Spread Adhesive Thickness and Surface on Strength and Stiffness of Joint, Proceedings 16th International Research/Expert Conference TMT 2012, 10-12 September 2012., Dubai, UAE, pp 571-574
[6] T. Mihailescu, An investigation of the performance of mortise and tenon joints using the finite element method, Journal of the Institute of Wood Science, Vol. 15 (2001), No. 5 (issue 89)
[7] C.A. Eckelman, S.K. Suddarth, Analysis and design of furniture frames, Wood Science and Technology, Vol. 3, No. 3 (1969), pp. 239-255.
[8] Y.Z. Erdil, A. Kasal, C.A. Eckelman, Bending moment capacity of rectangular mortise and tenon furniture joints, Forest Products Journal, Vol. 55, No. 12 (2005), pp. 209-213.
[9] S.Seker, A.U. Ozturk, C. Kozanoglu, Determination of reducing coefficient values of semi-rigid frames using artificial neural network, Mathematical and Computational Applications, Vol.16, No.3 (2011), pp. 649-658.
[10] T. J. Chung, Applied Continuum Mechanics, Cambridge University Press, Cambridge, 1996.
[11] J. Boding, B. A. Jayne, Mechanics of Wood and Wood Composites, Krieger publishing Company, Malabar Florida,1993.